ESC European Society of Cardiology

European Heart Journal - Imaging Methods and Practice (2025) **2**, qyaf033
https://doi.org/10.1093/ehjimp/qyaf033

ORIGINAL ARTICLE

Factors affecting the performance of a novel artificial intelligence-based coronary computed tomography-derived ischaemia algorithm

Peerapon Kiatkittikul [1,2], Teemu Maaniitty [1,3], Sarah Bär [1,4], Takeru Nabeta [5], Jeroen J. Bax [5,6], Antti Saraste [1,6], and Juhani Knuuti [1,3,*]

[1]Turku PET Centre, Turku University Hospital and University of Turku, P. O. Box 52, Turku FI-20521, Finland
[2]National Cyclotron and PET Centre, Chulabhorn Hospital, Chulabhorn Royal Academy, Bangkok, Thailand
[3]Department of Clinical Physiology, Nuclear Medicine, and PET, Turku University Hospital, Turku FI-20520, Finland
[4]Department of Cardiology, Bern University Hospital Inselspital, Bern, Switzerland
[5]Department of Cardiology, Leiden University Medical Center, Leiden, The Netherlands
[6]Heart Center, Turku University Hospital and University of Turku, Turku, Finland

Received 13 November 2024; accepted after revision 28 February 2025; online publish-ahead-of-print 17 April 2025

Abstract

Aims AI-QCT$_{ischaemia}$ is an FDA-cleared novel artificial intelligence–guided method that utilizes features from coronary computed tomography angiography (CCTA) to predict myocardial ischaemia.

Objective To identify factors associated with discrepancy between AI-QCT$_{ischaemia}$ and positron emission tomography (PET) perfusion.

Methods and results Six hundred and sixty-two patients with suspected obstructive coronary artery disease (CAD) on CCTA and undergoing [^{15}O]H_2O PET were analysed using AI-QCT$_{ischaemia}$. Multivariable logistic regression identified factors associated with discrepancy. Perfusion homogeneity was measured by relative flow reserve. A total of 209 (32%) patients showed discrepancies: 62 (9%) exhibited normal AI-QCT$_{ischaemia}$ but abnormal perfusion (false negative AI-QCT$_{ischaemia}$), whereas 147 (22%) had abnormal AI-QCT$_{ischaemia}$ despite normal perfusion (false positive AI-QCT$_{ischaemia}$). False positive AI-QCT$_{ischaemia}$ patients (vs. true positive) were more often females, older, with less typical angina, and less advanced CAD. In multivariable analysis, typical angina [OR 95% CI: 1.796 (1.015–3.179), $P = 0.044$], diameter stenosis per 1% increase [1.058 (1.036–1.080), $P < 0.001$], and percent atheroma volume per 1% increase [1.103 (1.051–1.158), $P < 0.001$] significantly predicted true positive, while age was inversely associated [0.955 (0.923–0.989), $P = 0.010$]. False-negative AI-QCT$_{ischaemia}$ patients (vs. true negative) were more often males, smokers, with less good CCTA image quality, and more advanced CAD. However, none was significant in multivariable analysis. Furthermore, false-negative AI-QCT$_{ischaemia}$ showed more homogenously reduced perfusion by relative flow reserve compared to true positive (median ± IQR: 0.68 ± 0.15 vs. 0.56 ± 0.23, $P < 0.001$) and 21 (34%) of false negative showed globally reduced perfusion.

Conclusion For abnormal AI-QCT$_{ischaemia}$, younger age, typical angina, more severe stenosis, and more extensive atherosclerosis predicted abnormal PET perfusion. With false negative AI-QCT$_{ischaemia}$, perfusion abnormalities were partly explained by microvascular disease.

* Corresponding author. E-mail: juhani.knuuti@utu.fi

Graphical Abstract

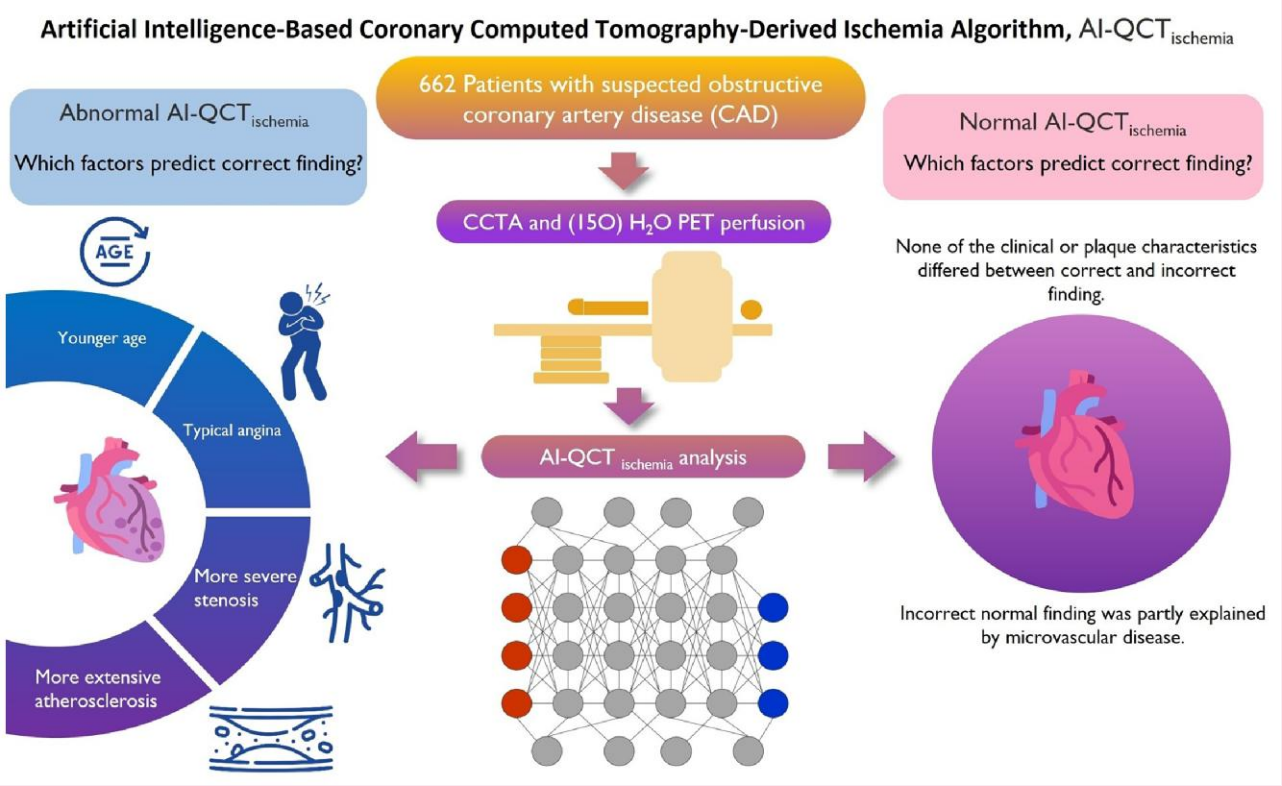

Keywords AI-QCT$_{ischaemia}$ • coronary computed tomography angiography • positron emission tomography • oxygen-15 water • coronary artery disease

Introduction

Coronary computed tomography angiography (CCTA) is one of the first-line non-invasive imaging modalities for the detection of coronary artery disease (CAD) among patients with low to intermediate pre-test probability of CAD.[1] Even though the sensitivity and negative predictive value of CCTA are high, the specificity and positive likelihood ratio are only moderate for the detection of functionally significant CAD defined by invasive fractional flow reserve (FFR).[2] Therefore, several computed tomography (CT) methods have been developed to improve the performance of CCTA, such as CCTA-based fractional flow reserve (FFR_{CT}) and CT myocardial perfusion imaging.[3]

Artificial intelligence (AI)-based methods for cardiovascular imaging have been developed in order to improve diagnostic performance and prognostic value of CCTA.[4] Recently, an AI-guided quantitative computed tomography (AI-QCT) has been shown to achieve improved accuracy for detection of obstructive stenosis, quantitation of atherosclerotic plaque burden, and assessing prognosis.[5,6] Furthermore, a novel AI-based quantitative computed tomography algorithm for predicting myocardial ischaemia (AI-QCT$_{ischaemia}$) has been developed and received clearance by the U.S. Food and Drug Administration (FDA) (Cleerly ISCHEMIA, Cleerly Inc, Denver CO, USA).[7] This algorithm utilizes 37 features from the AI-QCT algorithm related to coronary stenosis, vascular morphology, and plaque morphology to predict the probability of functionally significant CAD and was trained against invasive FFR. An external validation study showed that this algorithm has good diagnostic accuracy in predicting the presence of haemodynamically significant coronary stenosis defined by abnormal invasive FFR, with performance similar to [^{15}O]H_2O positron emission tomography (PET) myocardial perfusion imaging and superior to FFR_{CT}.[8] In addition, we and others have demonstrated the long-term prognostic value of AI-QCT$_{ischaemia}$ algorithm.[8,9] However, in our experience, discrepant results between AI-QCT$_{ischaemia}$ algorithm and PET myocardial perfusion imaging are not uncommon.[10] The present study aimed to investigate the factors that are associated with discrepant findings between AI-QCT$_{ischaemia}$ and PET myocardial perfusion imaging in patients with suspected obstructive CAD.

Methods

We reviewed all patients with clinically suspected CAD who underwent selective hybrid CCTA-PET at Turku PET Centre, Turku University Hospital (Turku, Finland) from February 2007 to December 2016. Patients with previously known CAD or evaluated due to heart failure or cardiomyopathy were not considered for inclusion. The study protocol was approved by the Ethics Committee of the Hospital District of Southwest Finland that waived the need for written informed consent due to retrospective observational study design.

A selective hybrid imaging protocol is routinely used in our hospital,[11] applying CCTA as a first-line imaging test. Downstream PET myocardial

perfusion imaging is performed to assess myocardial ischaemia if obstructive stenosis is suspected based on the initial visual interpretation of the CCTA images, using ≥50% diameter stenosis as a guideline. Therefore, this study focuses on patients who selectively underwent PET perfusion imaging due to suspected obstructive CAD on CCTA.

CCTA studies were performed with a 64-row PET/CT scanner (GE Discovery VCT or GE D690, General Electric Medical Systems, Waukesha, WI, USA) and using intravenously administered low-osmolal iodine contrast agents. Intravenous metoprolol (0–30 mg) was administered to reach a target heart rate of ≤60 bpm and short-acting oral nitrate was given for vasodilation. Prospectively electrocardiography-triggered acquisition was applied whenever feasible.

Myocardial perfusion PET imaging was acquired using the same scanner as CCTA and usually on the same day as CCTA. However, in some cases, PET imaging was performed within the following days or weeks due to logistic reasons or inadequate patient preparation. Patients abstained from caffeine for 24 h before the PET study. A dynamic stress-only PET perfusion scan with [^{15}O]H_2O tracer was performed during adenosine infusion (140 μg/kg/min), as previously described.[12] The PET data were analysed using Carimas software (Turku PET Centre, Turku, Finland). Absolute stress myocardial blood flow (sMBF) was quantified individually for the standard three main coronary territories (left anterior descending, left circumflex, right coronary artery) and for 17 myocardial segments. Abnormal perfusion on patient level was defined as sMBF ≤2.3 mL/g/min in at least 2 adjacent segments, excluding segments in the basal septal wall, a definition that has been derived and validated against invasive FFR with a cut-off of 0.80.[13] Regional ('defect') sMBF was calculated as an average sMBF of the two adjacent segments with the lowest flow. Relative flow reserve (RFR) was calculated as regional sMBF divided by the mean sMBF of a coronary territory with the highest flow.

AI-QCT$_{ischaemia}$ analysis

CCTA images were analysed by using an FDA-cleared AI-QCT algorithm (Cleerly LABS; Cleerly, Inc., Denver, CO, USA)[14,15] blinded to PET analysis results. The process involves generating a coronary artery centreline, contouring the lumen and outer vessel walls, and automated artery labelling based on their location.[15,16] The software provides multiple quantitative CT parameters, such as diameter stenosis degree (%), total plaque volume (mm^3), and percent atheroma volume (%). The output parameters from AI-QCT are then fed into AI-QCT$_{ischaemia}$ algorithm that determines the probability of myocardial ischaemia and provides a binary output: normal (ischaemia unlikely) vs. abnormal (ischaemia likely) (Cleerly ISCHEMIA, Cleerly, Inc., Denver, CO, USA).[8] The cut-off value (0.31) used for this binary classification has been previously optimized and validated against invasive FFR using cut-off 0.80.[8] Vessels with >15% of length having insufficient image quality as well as patients with coronary anomalies were deemed inconclusive. In this study we categorized patients as having (i) normal AI-QCT$_{ischaemia}$ when all vessels were classified as having ischaemia unlikely, (ii) abnormal AI-QCT$_{ischaemia}$ when there was at least one vessel with ischaemia likely, and (iii) inconclusive AI-QCT$_{ischaemia}$ when there was at least one inconclusive vessel in the absence of any ischaemic vessels.

Statistical analysis

All demographic and imaging data were analysed and reported as number (percentage) in categorical variables and median with interquartile range in non-parametric continuous variables. Chi-square test and Mann–Whitney *U* test were used for categorical and non-parametric continuous variables, respectively. Univariable and multivariable logistic regression analyses were used to find the variables associated with a discrepant perfusion result in each AI-QCT$_{ischaemia}$ subgroup (normal vs. abnormal). Demographic and imaging variables were included in the regression models, except regional myocardial blood flow because this variable is directly linked to the PET perfusion findings. In addition, percent atheroma volume was used to represent plaque burden in the models. *P*-value ≤ 0.05 was considered statistically significant. The variables with significant (*P*-value ≤ 0.05) association on univariable logistic regression analysis were included in the multivariable logistic regression analysis model. All statistical analyses were conducted using IBM SPSS Statistics for Windows, version 28.0 (IBM Corp., Armonk, New York, USA).

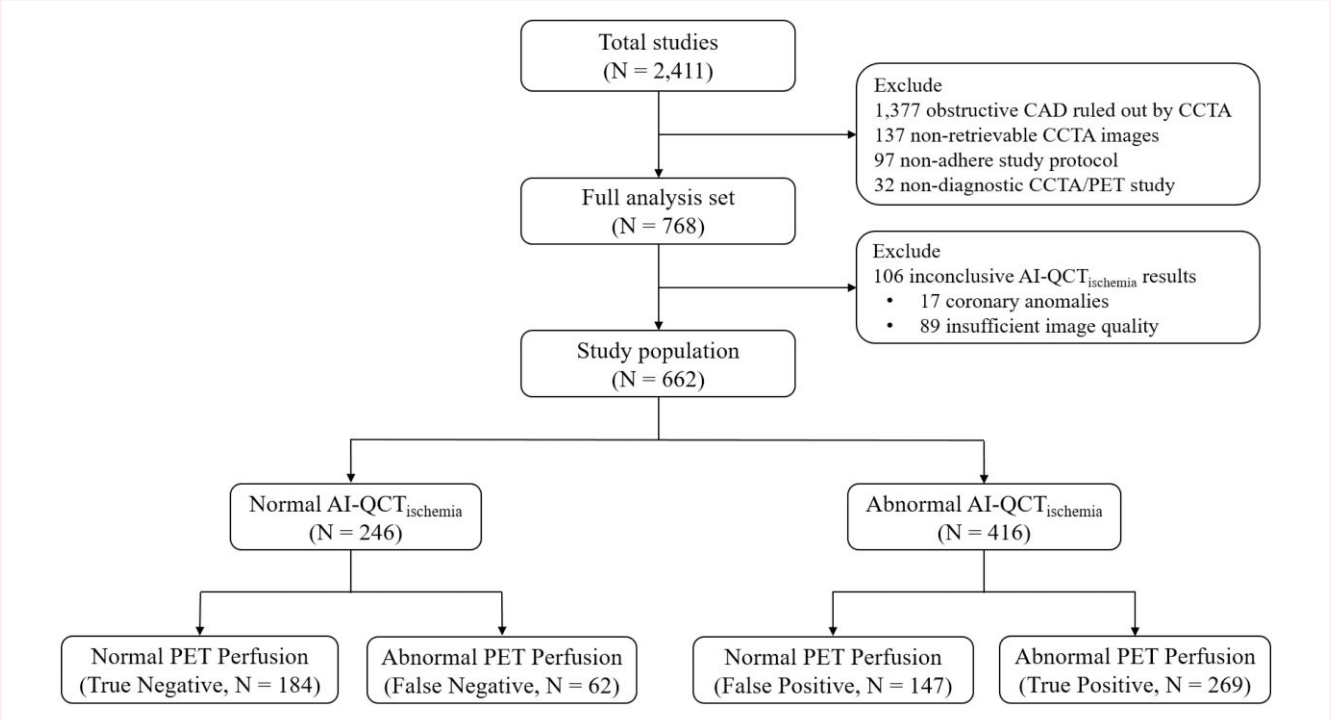

Figure 1 Study flow chart shows the enrolment process and number of patients in this study. CAD, coronary artery disease; CCTA, coronary computed tomography angiography; PET, positron emission computed tomography.

Results

In total, 2411 consecutive symptomatic patients underwent CCTA for suspected CAD, out of whom 1377 had obstructive CAD ruled out by CCTA and therefore did not undergo PET perfusion imaging. Moreover, 137 had non-retrievable CCTA images, 97 did not adhere to the selective hybrid imaging protocol (i.e. no PET perfusion imaging despite obstructive stenosis on CCTA), and 32 had non-diagnostic CCTA/PET study. After these exclusions, there remain 768 patients who underwent [^{15}O]H_2O PET due to suspected obstructive CAD on CCTA, constituting the full analysis set of this study.

Out of these, 106 (14%) patients were further excluded due to inconclusive AI-QCT$_{ischaemia}$ results, including 17 patients with coronary anomalies, and 89 patients excluded for insufficient image quality. More specifically, the unevaluable vessels included 57 (39%) right coronary arteries, 47 (34%) left circumflex arteries, and 40 (27%) left anterior descending arteries. Among the patients with inconclusive AI-QCT$_{ischaemia}$ algorithm, 42 (40%) had abnormal PET perfusion.

The final study cohort included 662 patients, who had suspected obstructive CAD in CCTA, underwent PET perfusion imaging, and had conclusive AI-QCT$_{ischaemia}$ results (*Figure 1*). Four hundred fifty-three (68%) patients had concordant findings by both methods and 209 (32%) patients had discrepant findings. The patients were classified into (i) normal AI-QCT$_{ischaemia}$ with normal perfusion (true negative AI-QCT$_{ischaemia}$, TN group, $n = 184$), (ii) normal AI-QCT$_{ischaemia}$ with abnormal perfusion (false negative AI-QCT$_{ischaemia}$, FN group, $n = 62$), (iii) abnormal AI-QCT$_{ischaemia}$ with normal perfusion (false positive AI-QCT$_{ischaemia}$, FP group, $n = 147$), and (iv) abnormal AI-QCT$_{ischaemia}$ with abnormal perfusion (true positive AI-QCT$_{ischaemia}$, TP group, $n = 269$; *Figure 2*).

Discrepant findings in patients with abnormal AI-QCT$_{ischaemia}$

In 416 patients with abnormal AI-QCT$_{ischaemia}$, PET perfusion was normal in 147 (35%) and abnormal in 269 (65%) patients. Therefore, in 22% of the study cohort, AI-QCT$_{ischaemia}$ was classified as false positive (*Figure 2*). The false positive AI-QCT$_{ischaemia}$ finding (vs. true positive) was more common in females and those with less typical angina (*Table 1*). In addition, false positive AI-QCT$_{ischaemia}$ finding was associated with lower total calcium score (*Figure 3A*), lower diameter stenosis (*Figure 3B*), smaller total plaque volume, smaller percent atheroma volume (*Figure 3C*), and older age (*Figure 3D*). The probability of ischaemia by AI-QCT$_{ischaemia}$ algorithm was also lower in those with normal PET perfusion than in those with abnormal PET perfusion (*Table 1*).

In univariable logistic regression analysis male sex, age, typical angina, total calcium score, diameter stenosis, and percent atheroma volume were significantly associated with a true positive AI-QCT$_{ischaemia}$ finding. In multivariable analysis, only typical angina, increasing diameter stenosis, and increasing percent atheroma volume were predictors of true positive AI-QCT$_{ischaemia}$ finding with adjusted odds ratios (OR) ([95%C.I.], *P*-value) of 1.796 ([1.015–3.179], 0.044), 1.058 ([1.036–1.080], < 0.001)

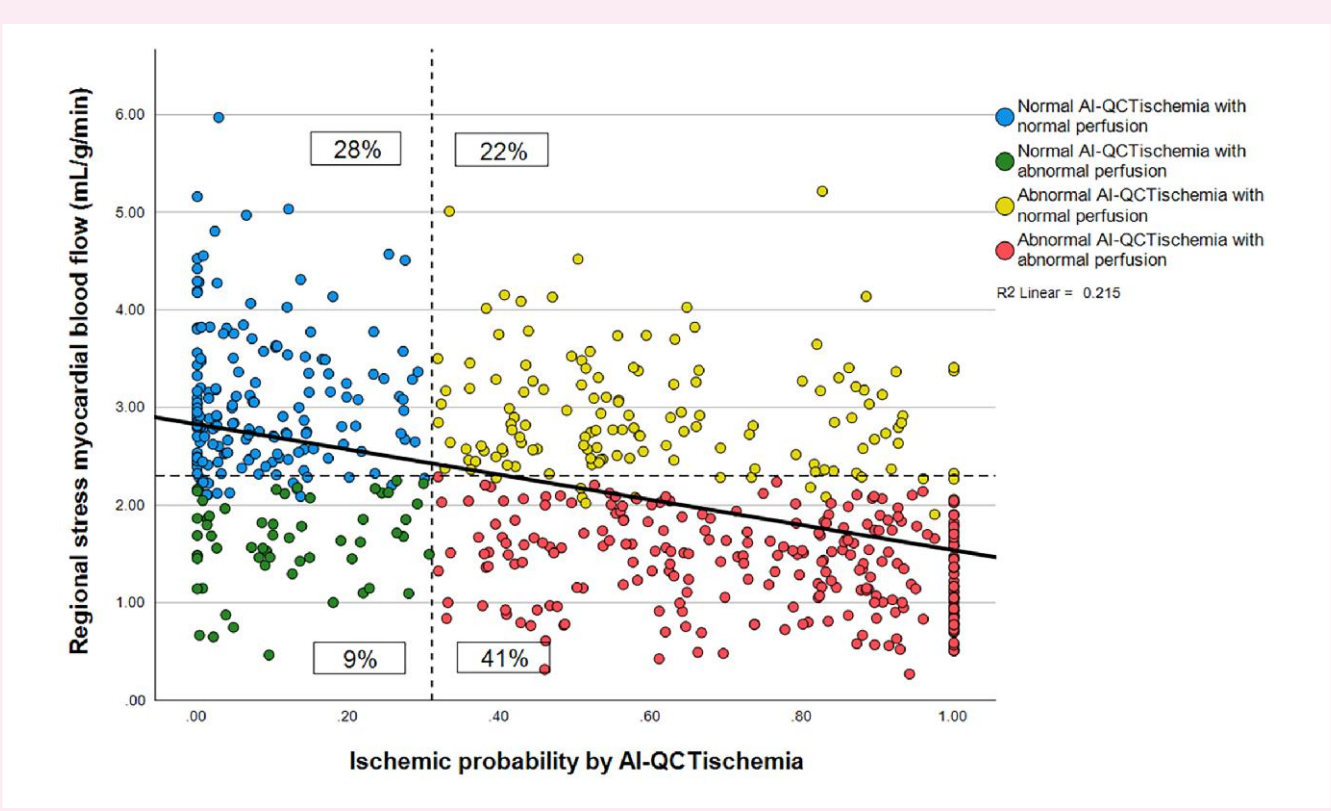

Figure 2 Scatter plot of regional stress myocardial blood flow and likelihood of ischaemia based on AI-QCT$_{ischaemia}$. The dotted lines represent the cut-off value to discriminate normal and abnormal result in both tests and the black line is the linear fit line, representing the correlation between these tests. Four discrete groups were classified according to the results: (i) normal AI-QCT$_{ischaemia}$ with normal perfusion (TN, blue, $n = 184$, 28%), (ii) normal AI-QCT$_{ischaemia}$ with abnormal perfusion (FN, green, $n = 62$, 9%), (iii) abnormal AI-QCT$_{ischaemia}$ with normal perfusion (FP, yellow, $n = 147$, 22%), and (iv) abnormal AI-QCT$_{ischaemia}$ with abnormal perfusion (TP, red, $n = 269$, 41%). Some patients classified as having normal perfusion (blue and yellow) appear to have regional stress myocardial blood flow ≤2.3 mL/g/min as it was calculated as an average of two adjacent segments, but do not fulfil the criterion of having two adjacent abnormal segments.

per 1% increase, and 1.103 ([1.051–1.158], < 0.001) per 1% increase, respectively (*Table 2*). The age was inversely associated with true positive AI-QCT$_{ischaemia}$ finding, i.e. the older patients had more commonly discrepant finding (false positive), with adjusted OR [(95% CI), *P*-value] of 0.955 [(0.923–0.989), 0.010] per 1-year increase.

Discrepant findings in patients with normal AI-QCT$_{ischaemia}$

In 246 patients with normal AI-QCT$_{ischaemia}$, PET perfusion was normal in 184 (75%) and abnormal in 62 (25%) patients (*Table 1*). Therefore, in 9% of the study cohort, AI-QCT$_{ischaemia}$ was classified as false negative due to abnormal PET perfusion (*Figure 2*). The false negative AI-QCT$_{ischaemia}$ finding was more common in males and associated with smoking, total calcium score (*Figure 3A*), diameter stenosis (*Figure 3B*), total plaque volume, percent atheroma volume (*Figure 3C*), and impaired CCTA image quality (*Table 1*).

Univariable logistic regression analysis showed that male sex, smoking, less good CCTA image quality, total calcium score, diameter stenosis, and percent atheroma volume were significantly predicted false negative AI-QCT$_{ischaemia}$ findings (abnormal perfusion). However, significant associations could not be demonstrated in multivariable analysis (*Table 3*).

Relative flow reserve and AI-QCT$_{ischaemia}$

Relative flow reserve as a measure of regional myocardial perfusion homogeneity was higher in patients with normal perfusion as compared to abnormal perfusion group (median ± IQR of 0.73 ± 0.12 and 0.59 ± 0.24, respectively, $P < 0.001$). In patients with normal perfusion, there was no significant difference in relative flow reserve between those with true negative and false positive AI-QCT$_{ischaemia}$ findings (median ± IQR of 0.73 ± 0.11 and 0.73 ± 0.14, respectively, $P = 0.661$). In patients with abnormal perfusion, those with false negative AI-QCT$_{ischaemia}$ had significantly higher relative flow reserve as compared to group with true positive AI-QCT$_{ischaemia}$ (median ± IQR of 0.68 ± 0.15 and 0.56 ± 0.23, respectively, $P < 0.001$). In patients with normal AI-QCT$_{ischaemia}$, but abnormal perfusion (false negative AI-QCT$_{ischaemia}$ finding), 21 (34%) out of 62 patients had abnormal myocardial perfusion involving all three main coronary territories, suggesting microvascular disease.

Discussion

Recently, an AI-based algorithm, AI-QCT$_{ischaemia}$, was developed to predict myocardial ischaemia utilizing CCTA-derived morphologic features such as coronary stenosis, vascular morphology, and plaque morphology. A recent validation study[8] showed that AI-QCT$_{ischaemia}$ algorithm has good diagnostic accuracy in predicting the presence of haemodynamically significant coronary stenosis defined by abnormal invasive FFR, with comparable diagnostic performance as PET myocardial perfusion imaging. Still, discrepant findings between AI-QCT$_{ischaemia}$ algorithm and PET perfusion imaging seem to be not uncommon.[10] The goals of this study were to evaluate how often there are discrepant findings between AI-QCT$_{ischaemia}$ algorithm and quantitative PET myocardial perfusion imaging and to identify factors that are associated with the discrepant findings.

The AI-QCT$_{ischaemia}$ algorithm predicts the probability of functionally significant CAD based on 37 CCTA-derived parameters beyond commonly used percent diameter stenosis in the interpretation of CCTA, as prior studies have found that higher coronary plaque burden is associated with a higher risk of myocardial ischaemia.[17,18] Still, it is not surprising to find discrepancies between AI-QCT$_{ischaemia}$ and PET

Table 1 Demographic data and imaging results

Variables	Normal AI-QCT$_{ischaemia}$ (246)			Abnormal AI-QCT$_{ischaemia}$ (416)		
	Normal perfusion (184) (True negative)	Abnormal perfusion (62) (False negative)	*P*-value	Normal perfusion (147) (False positive)	Abnormal perfusion (269) (True positive)	*P*-value
Male sex	**86 (47%)**	**40 (65%)**	**0.019**	**71 (48%)**	**188 (70%)**	**<0.001**
Age (year)	66 ± 13	65 ± 12	0.314	**68 ± 9**	**66 ± 11**	**0.001**
BMI (kg/m^2, $n = 612$)	27.3 ± 6.1	26.6 ± 5	0.596	27.5 ± 5.3	27.7 ± 6.0	0.770
Smoking	**67 (36%)**	**32 (52%)**	**0.037**	58 (39%)	115 (43%)	0.534
Diabetes	33 (18%)	9 (14%)	0.697	33 (22%)	61 (23%)	1.000
Hypertension	119 (65%)	42 (68%)	0.758	109 (74%)	182 (68%)	0.181
Dyslipidaemia	127 (69%)	42 (74%)	0.521	105 (71%)	203 (75%)	0.413
Family history of CAD	81 (44%)	33 (53%)	0.240	70 (48%)	119 (44%)	0.537
Typical angina	42 (23%)	19 (31%)	0.236	**33 (22%)**	**91 (34%)**	**0.018**
Dyspnoea	68 (37%)	26 (42%)	0.546	61 (41%)	106 (39%)	0.677
Atrial fibrillation or flutter	18 (10%)	2 (3%)	0.115	14 (9%)	23 (9%)	0.723
Excellent or good CCTA quality ($n = 607$)	**137 (74%)**	**37 (60%)**	**0.041**	165 (61%)	91 (62%)	0.910
Total calcium score ($n = 561$)	**124 ± 227**	**194 ± 556**	**0.036**	**406 ± 768**	**655 ± 1128**	**0.009**
Regional myocardial blood flow (mL/g/min, $n = 628$)	**2.9 ± 0.9**	**1.7 ± 0.5**	**<0.001**	**2.8 ± 0.8**	**1.4 ± 0.7**	**<0.001**
Diameter stenosis (%)[a]	**31 ± 18**	**36 ± 16**	**0.032**	**59 ± 17**	**72 ± 19**	**<0.001**
Total plaque volume (mm^3)[a]	**194 ± 189**	**281 ± 356**	**0.004**	**407 ± 477**	**568 ± 567**	**<0.001**
Percent atheroma volume (%)[a]	**6 ± 6**	**8 ± 9**	**0.004**	**14 ± 12**	**19 ± 16**	**<0.001**
Ischaemic probability by AI-QCT$_{ischaemia}$	0.05 ± 0.14	0.09 ± 0.19	0.074	**0.55 ± 0.38**	**0.83 ± 0.36**	**<0.001**

BMI, body mass index; CAD, coronary artery disease; CCTA, coronary computed tomography angiography.
Bold text is for statistical significant.
[a]Originated from AI-QCT algorithm.

perfusion. First, the relationship between anatomical and functional characteristics of a coronary stenosis is complex, and AI-QCT$_{ischaemia}$ algorithm relies on anatomical CCTA data. Second, myocardial perfusion by PET is determined not only by the resistance of epicardial coronary arteries but also by coronary microvasculature.

To determine the factors that are potentially associated with the discrepancies, we focused on patients with false positive or false negative findings. In patients with abnormal AI-QCT$_{ischaemia}$ results, multivariable analysis showed that typical angina, increasing diameter stenosis, increasing percent atheroma volume, and younger age independently predicted true positive results (*Table 2*). Thus, as expected, higher diameter stenosis and more typical angina have a higher probability of CAD from AI-QCT$_{ischaemia}$ algorithm and a higher chance of abnormal perfusion, leading to concordant result.[19–22]

We also noted that the patients with higher percent atheroma volume had a higher proportion of true positive AI-QCT$_{ischaemia}$ results (*Figure 3C*). Percent atheroma volume represents the amount of atherosclerotic plaque in the coronary arteries. Min *et al.*[6] demonstrated that ischaemic patients based on FFR had higher percent atheroma volume as compared to non-ischaemic patients. A higher percent atheroma volume also independently predicted myocardial ischaemia by using functional imaging as a reference standard.[23] Both diameter stenosis and plaque volume are features included in AI-QCT$_{ischaemia}$ algorithm.[8] False positive AI-QCT$_{ischaemia}$ findings were more prominent among patients older than 80 years (*Figure 3D*). This could be associated with the previous findings[24,25] that higher age was associated with more diffuse atherosclerosis.[26,27]

In patients with normal AI-QCT$_{ischaemia}$ results, univariable analysis showed that male sex, smoking, less good CCTA image quality, total calcium score, diameter stenosis, and percent atheroma volume were significantly associated with false-negative AI-QCT$_{ischaemia}$ findings. However, significant associations could not be demonstrated in multivariable analysis (*Table 3*). An interesting finding was that the patients with false negative AI-QCT$_{ischaemia}$ had higher relative flow reserve, i.e. the perfusion was abnormal but less heterogeneous as compared with true positive findings. Diffused reduction of myocardial blood flow is a typical finding in patients with microvascular disease.[28] Indeed, myocardial blood flow was impaired globally (in all three coronary territories) in about 34% of patients with false negative AI-QCT$_{ischaemia}$ findings. This is expected as epicardial disease does not explain abnormal perfusion in these patients. Microvascular disease is characterized by abnormalities in the coronary arterioles and capillaries resulting in dysfunction of coronary microcirculation. Microvascular disease is often responsible for myocardial ischaemia without evidence of significant obstructive CAD and associated with an increased risk of cardiovascular events such as unstable angina, myocardial infarction, and cardiac death.[29] In contrast, among patients with normal perfusion, relative flow reserve did not differ between false positive and true negative cases, a finding that was against our hypothesis that more advanced CAD features (causing false positive AI-QCT$_{ischaemia}$ finding) would result in more heterogeneity in myocardial blood flow and reduced relative flow reserve (despite preserved absolute blood flow). It should be acknowledged that our selective hybrid CCTA/PET imaging protocol is limited in detecting pure coronary microvascular dysfunction because only patients with suspected obstructive stenosis on CCTA are referred to downstream PET perfusion imaging. However, our approach is well in agreement with the recent European guidelines[1] that suggest sequential testing in the diagnostic work-up of CAD. The patients included in our analysis

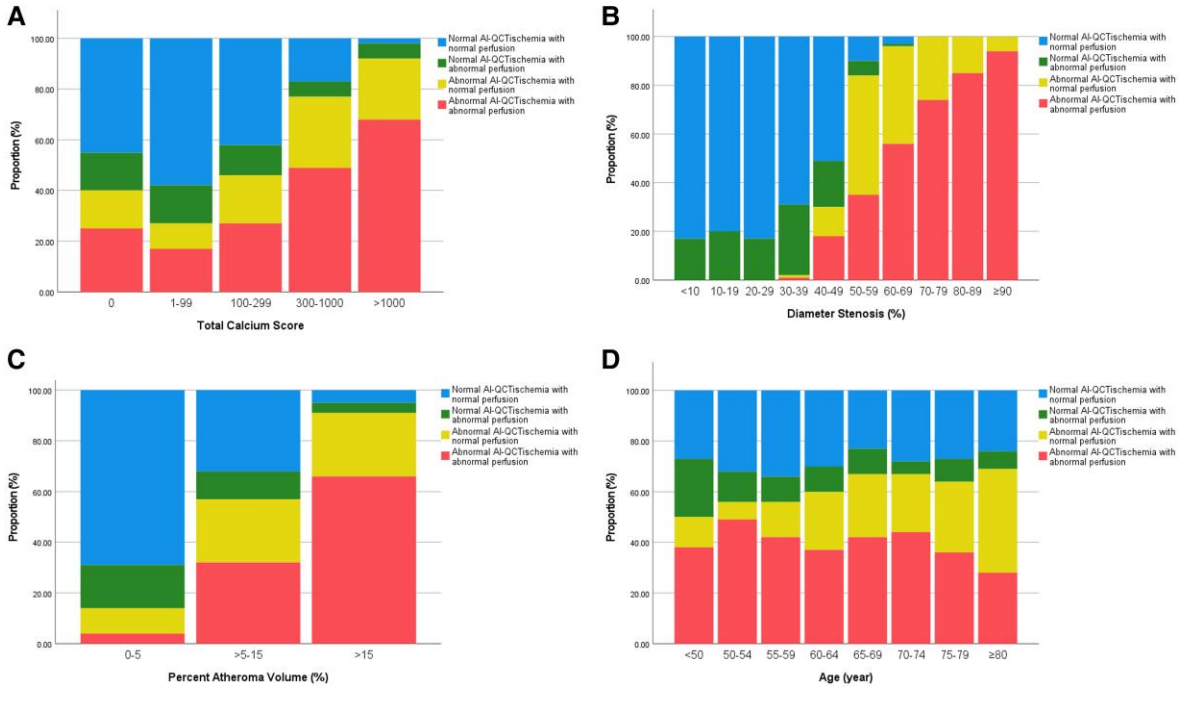

Figure 3 Proportion bar graphs of patients classified by total calcium score (*A*), diameter stenosis (*B*), percent atheroma volume (*C*), and age (*D*). The proportion of abnormal AI-QCT$_{ischaemia}$ with abnormal perfusion patients (TP, red) gradually increased in more advanced disease as defined by total calcium score (*A*), diameter stenosis (*B*), and percent atheroma volume (*C*). In contrast, the proportion of normal AI-QCT$_{ischaemia}$ with normal perfusion patients (TN, blue) gradually decreased with more advanced disease. The proportions of discrepant results (FN, green and FP, yellow) were almost equal in each severity grade of total calcium score (*A*) and percent atheroma volume (*C*), while the discrepancy rate is highest in 50–59% range of diameter stenosis (*B*). For age (*D*), the discrepancy rate is highest in those aging more than 80 years.

Table 2 Univariable and multivariable logistic regression analysis for predicting abnormal perfusion (concordance) in abnormal AI-QCT$_{ischaemia}$

Demographic and imaging variables ($n = 416$)	Univariable analysis		Multivariable analysis	
	Unadjusted OR (95% C.I.)	*P*-value	Adjusted OR (95% C.I.)	*P*-value
Male sex	**2.484 (1.640–3.764)**	**<0.001**	1.494 (0.884–2.526)	0.134
Age (per 1 year increase)	**0.957 (0.932–0.982)**	**<0.001**	**0.955 (0.923–0.989)**	**0.010**
BMI (per 1 kg/m^2 increase)	1.003 (0.959–1.049)	0.905	—	—
Smoking	1.146 (0.761–1.726)	0.515	—	—
Diabetes	1.013 (0.626–1.639)	0.958	—	—
Hypertension	0.729 (0.465–1.143)	0.168	—	—
Dyslipidaemia	1.230 (0.782–1.935)	0.370	—	—
Family history of CAD	0.873 (0.583–1.306)	0.508	—	—
Typical angina	**1.766 (1.112–2.805)**	**0.016**	**1.796 (1.015–3.179)**	**0.044**
Dyspnoea	0.917 (0.609–1.380)	0.677	—	—
Atrial fibrillation or flutter	0.888 (0.442–1.783)	0.739	—	—
Excellent or good CCTA quality	1.030 (0.661–1.604)	0.891	—	—
Total calcium score (per 10-unit increase)	**1.004 (1.001–1.007)**	**0.006**	0.997 (0.992–1.002)	0.249
Diameter stenosis (per 1% increase)[a]	**1.059 (1.041–1.077)**	**<0.001**	**1.058 (1.036–1.080)**	**<0.001**
Percent atheroma volume (per 1% increase)[a]	**1.051 (1.028–1.076)**	**<0.001**	**1.103 (1.051–1.158)**	**<0.001**

BMI, body mass index; CAD, coronary artery disease; CCTA, coronary computed tomography angiography; OR, odds ratio.
Bold text is for statistical significant.
[a]Originated from AI-QCT algorithm.

Table 3 Univariable and multivariable logistic regression analysis for predicting abnormal perfusion (discordance) in normal AI-QCT$_{ischaemia}$

Demographic and imaging variables ($n = 246$)	Univariable analysis		Multivariable analysis	
	Unadjusted OR (95% CI)	*P*-value	Adjusted OR (95% CI)	*P*-value
Male sex	**2.072 (1.142–3.758)**	**0.016**	1.910 (0.897–4.067)	0.093
Age (per 1 year increase)	0.978 (0.947–1.010)	0.183	—	—
BMI (per 1 kg/m^2 increase)	0.996 (0.939–1.057)	0.898	—	—
Smoking	**1.863 (1.041–3.332)**	**0.036**	1.329 (0.635–2.783)	0.451
Diabetes	0.777 (0.349–1.731)	0.537	—	—
Hypertension	1.147 (0.622–2.116)	0.661	—	—
Dyslipidaemia	1.290 (0.674–2.469)	0.441	—	—
Family history of CAD	1.447 (0.812–2.578)	0.210	—	—
Typical angina	1.494 (0.787–2.834)	0.219	—	—
Dyspnoea	1.232 (0.685–2.215)	0.486	—	—
Atrial fibrillation or flutter	0.307 (0.069–1.365)	0.121	—	—
Excellent or good CCTA quality	**0.480 (0.243–0.950)**	**0.035**	1.008 (0.995–1.022)	0.212
Total calcium score (per 10-unit increase)	**1.015 (1.006–1.025)**	**0.002**	0.586 (0.262–1.312)	0.194
Diameter stenosis (per 1% increase)[a]	**1.025 (1.001–1.050)**	**0.039**	0.999 (0.966–1.034)	0.976
Percent atheroma volume (per 1% increase)[a]	**1.094 (1.041–1.150)**	**<0.001**	1.028 (0.927–1.139)	0.600

BMI, body mass index; CAD, coronary artery disease; CCTA, coronary computed tomography angiography; OR, odds ratio.
Bold text is for statistical significant.
[a]Originated from AI-QCT algorithm.

($n = 662$) represent those who need downstream functional testing after first-line CCTA.

Both AI-QCT$_{ischaemia}$ (using cut-off 0.31 for binary classification) and [^{15}O]H_2O PET myocardial perfusion imaging (using cut-off 2.3 mL/g/min) have been derived and validated against invasive FFR with a cut-off of 0.80, although AI-QCT$_{ischaemia}$ is based on anatomical status of coronary arteries whereas PET perfusion is truly functional and integrates both epicardial and microvascular coronary circulation. Myocardial perfusion imaging with [^{15}O]H_2O PET has been clinically used for >15 years and was used as a reference standard in the present

analysis, although we recognize that all methods have their inherent strengths and limitations. A good example of this is the patients with microvascular disease, who may show a normal AI-QCT$_{ischaemia}$ finding and normal invasive FFR but abnormal myocardial perfusion.

Conclusion

We identified factors that are associated with discrepant findings between AI-QCT$_{ischaemia}$ algorithm and PET myocardial perfusion imaging. We found false positive AI-QCT$_{ischaemia}$ finding in 22% of patients and these appear to be associated with age, type of symptoms, and CCTA features such as diameter stenosis and percent atheroma volume. The false negative AI-QCT$_{ischaemia}$ findings are associated with more homogeneously reduced myocardial perfusion which might be partly related to coronary microvascular dysfunction.

Funding

The study was financially supported by the Finnish Foundation for Cardiovascular Research and Finnish State Research Funding [VTR 13403]. Dr Kiatkittikul was supported by Chulabhorn Royal Academy. Cleerly, Inc. performed the CCTA image analysis without costs and provided an unrestricted grant to the research team.

Conflict of interest: P.K. reports research grants support from Chulabhorn Royal Academy (Bangkok, Thailand). S.B. reports personal research grants from the Swiss National Science Foundation, and the University of Turku, Finland; and research grants to the institution from Medis Medical Imaging Systems, Bangerter-Rhyner Stiftung (Basel, Switzerland), Abbott, outside the submitted work. A.S. received consultancy fees from Astra Zeneca and Pfizer, and speaker fees from Abbott, Astra Zeneca, BMS, Janssen, Novartis, and Pfizer. J.J.B. received speaker fees from Abbott. J.K. received consultancy fees from GE Healthcare and Synektik and speaker fees from Bayer, Lundbeck, Boehringer-Ingelheim, Pfizer, and Siemens, outside of the submitted work. All other authors have reported that they have no relationships relevant to the contents of this paper to disclose.

Data availability

The data underlying this article will be shared on reasonable request to the corresponding author.

Lead author biography

Peerapon Kiatkittikul, M.D., is a nuclear medicine physician working at the National Cyclotron and PET Centre, Chulabhorn Hospital, part of the Chulabhorn Royal Academy in Thailand. He is also work as a research fellow at the Turku PET Centre in Finland, focusing on the advance imaging technique to improve the diagnosis of the cardiovascular disease.

References

1. Vrints C, Andreotti F, Koskinas KC, Rossello X, Adamo M, Ainslie J *et al.* 2024 ESC guidelines for the management of chronic coronary syndromes. *Eur Heart J* 2024;**45**:3415–537.
2. Knuuti J, Ballo H, Juarez-Orozco LE, Saraste A, Kolh P, Rutjes AWS *et al.* The performance of non-invasive tests to rule-in and rule-out significant coronary artery stenosis in patients with stable angina: a meta-analysis focused on post-test disease probability. *Eur Heart J* 2018;**39**:3322–30.
3. Gonzalez JA, Lipinski MJ, Flors L, Shaw PW, Kramer CM, Salerno M. Meta-analysis of diagnostic performance of coronary computed tomography angiography, computed tomography perfusion, and computed tomography-fractional flow reserve in functional myocardial ischemia assessment versus invasive fractional flow reserve. *Am J Cardiol* 2015;**116**:1469–78.
4. Slart RHJA, Williams MC, Juarez-Orozco LE, Rischpler C, Dweck MR, Glaudemans AWJM *et al.* Position paper of the EACVI and EANM on artificial intelligence applications in multimodality cardiovascular imaging using SPECT/CT, PET/CT, and cardiac CT. *Eur J Nucl Med Mol Imaging* 2021;**48**:1399–413.
5. Lipkin I, Telluri A, Kim Y, Sidahmed A, Krepp JM, Choi BG *et al.* Coronary CTA with AI-QCT interpretation: comparison with myocardial perfusion imaging for detection of obstructive stenosis using invasive angiography as reference standard. *AJR Am J Roentgenol* 2022;**219**:407–19.
6. Min JK, Chang HJ, Andreini D, Pontone G, Guglielmo M, Bax JJ *et al.* Coronary CTA plaque volume severity stages according to invasive coronary angiography and FFR. *J Cardiovasc Comput Tomogr* 2022;**16**:415–22.
7. Cleerly Launches Cleerly ISCHEMIA Solution for Heart Disease Analysis [Internet]. [cited 2025 Mar 28]. Available from: https://cleerlyhealth.com/press/cleerly-launches-ischemia-heart-disease-analysis.
8. Nurmohamed NS, Danad I, Jukema RA, de Winter RW, de Groot RJ, Driessen RS *et al.* Development and validation of a quantitative coronary CT angiography model for diagnosis of vessel-specific coronary ischemia. *JACC Cardiovasc Imaging* 2024;**17**:894–906.
9. Bär S, Nabeta T, Maaniitty T, Saraste A, Bax JJ, Earls JP *et al.* Prognostic value of a novel artificial intelligence-based coronary computed tomography angiography-derived ischaemia algorithm for patients with suspected coronary artery disease. *Eur Heart J Cardiovasc Imaging* 2024;**25**:657–67.
10. Nabeta T, Bär S, Maaniitty T, Min JK, Earls JP, Bax JJ *et al.* Incremental value of a novel AI-based CCTA derived ischemia algorithm over standard CCTA interpretation for predicting myocardial ischemia in suspected coronary artery disease. *European Heart Journal* 2023; **44**(Supplement_2):ehad655.149.
11. Maaniitty T, Stenström I, Bax JJ, Uusitalo V, Ukkonen H, Kajander S *et al.* Prognostic value of coronary CT angiography with selective PET perfusion imaging in coronary artery disease. *JACC Cardiovasc Imaging* 2017;**10**:1361–70.
12. Kajander S, Joutsiniemi E, Saraste M, Pietilä M, Ukkonen H, Saraste A *et al.* Cardiac positron emission tomography/computed tomography imaging accurately detects anatomically and functionally significant coronary artery disease. *Circulation* 2010;**122**:603–13.
13. Danad I, Uusitalo V, Kero T, Saraste A, Raijmakers PG, Lammertsma AA *et al.* Quantitative assessment of myocardial perfusion in the detection of significant coronary artery disease: cutoff values and diagnostic accuracy of quantitative [15O]H2O PET imaging. *J Am Coll Cardiol* 2014;**64**:1464–75.
14. Choi AD, Marques H, Kumar V, Griffin WF, Rahban H, Karlsberg RP *et al.* CT evaluation by artificial intelligence for atherosclerosis, stenosis and vascular morphology (CLARIFY): a multi-center, international study. *J Cardiovasc Comput Tomogr* 2021;**15**:470–6.
15. Griffin WF, Choi AD, Riess JS, Marques H, Chang HJ, Choi JH *et al.* AI evaluation of stenosis on coronary CTA, comparison with quantitative coronary angiography and fractional flow reserve: a CREDENCE trial substudy. *JACC Cardiovasc Imaging* 2023;**16**:193–205.
16. Singh G, Al'Aref SJ, Van Assen M, Kim TS, van Rosendael A, Kolli KK *et al.* Machine learning in cardiac CT: basic concepts and contemporary data. *J Cardiovasc Comput Tomogr* 2018;**12**:192–201.
17. Driessen RS, Stuijfzand WJ, Raijmakers PG, Danad I, Min JK, Leipsic JA *et al.* Effect of plaque burden and morphology on myocardial blood flow and fractional flow reserve. *J Am Coll Cardiol* 2018;**71**:499–509.
18. Eskerud I, Gerdts E, Larsen TH, Simon J, Maurovich-Horvat P, Lønnebakken MT. Total coronary atherosclerotic plaque burden is associated with myocardial ischemia in non-obstructive coronary artery disease. *Int J Cardiol Heart Vasc* 2021;**35**:100831.
19. de Waard GA, Cook CM, van Royen N, Davies JE. Coronary autoregulation and assessment of stenosis severity without pharmacological vasodilation. *Eur Heart J* 2018;**39**:4062–71.
20. Nijjer SS, de Waard GA, Sen S, van de Hoef TP, Petraco R, Echavarría-Pinto M *et al.* Coronary pressure and flow relationships in humans: phasic analysis of normal and pathological vessels and the implications for stenosis assessment: a report from the Iberian-Dutch-English (IDEAL) collaborators. *Eur Heart J* 2016;**37**:2069–80.
21. Lee JM, Hwang D, Park J, Zhang J, Tong Y, Kim CH *et al.* Exploring coronary circulatory response to stenosis and its association with invasive physiologic indexes using absolute myocardial blood flow and coronary pressure. *Circulation* 2017;**136**:1798–808.
22. Genders TSS, Steyerberg EW, Hunink MGM, Nieman K, Galema TW, Mollet NR *et al.* Prediction model to estimate presence of coronary artery disease: retrospective pooled analysis of existing cohorts. *BMJ* 2012;**344**:e3485.
23. Bakhshi H, Meyghani Z, Kishi S, Magalhães TA, Vavere A, Kitslaar PH *et al.* Comparative effectiveness of CT-derived atherosclerotic plaque metrics for predicting myocardial ischemia. *JACC Cardiovasc Imaging* 2019;**12**(7 Pt 2):1367–76.

24. Beverly J, Budoff MJ. Use of coronary computed tomography for calcium screening of atherosclerosis. *Heart Int* 2020;**14**:76–9.
25. Jonas R, Earls J, Marques H, Chang HJ, Choi JH, Doh JH *et al.* Relationship of age, atherosclerosis and angiographic stenosis using artificial intelligence. *Open Heart* 2021;**8**: e001832.
26. Onnis C, Virmani R, Kawai K, Nardi V, Lerman A, Cademartiri F *et al.* Coronary artery calcification: current concepts and clinical implications. *Circulation* 2024;**149**:251–66.
27. Williams MC, Moss AJ, Dweck M, Adamson PD, Alam S, Hunter A *et al.* Coronary artery plaque characteristics associated with adverse outcomes in the SCOT-HEART study. *J Am Coll Cardiol* 2019;**73**:291–301.
28. Schindler TH, Dilsizian V. Coronary microvascular dysfunction: clinical considerations and noninvasive diagnosis. *JACC Cardiovasc Imaging* 2020;**13**(1 Pt 1):140–55.
29. Varrichione G, Biccirè FG, Di Pietro R, Prati F, Battisti P. The risk of acute coronary events in microvascular disease. *Eur Heart J Suppl* 2022;**24**(Suppl I):I127–30.